DAMAGE INSPECTION OF WIPER BLADES USING IMAGE PROCESSING TECHNIQUES

Hoang Thai Son Nguyen[1], Duy Anh Nguyen[2], and Tan Tien Nguyen[3]

[1] Hi-Tech Mechatronics Laboratory, Faculty of Mechanical Engineer, Ho Chi Minh City University of Technology, Ho Chi Minh City, Vietnam, e-mail: sonnguye@gmail.com

[2] Mechatronics Engineering Deptartment, Faculty of Mechanical Engineer, Ho Chi Minh City University of Technology, Ho Chi Minh City, Vietnam, e-mail:duyanhnguyen@hcmut.edu.vn

[3] Mechatronics Engineering Deptartment, Faculty of Mechanical Engineer, Ho Chi Minh City University of Technology, Ho Chi Minh City, Vietnam, e-mail:nttien@hcmut.edu.vn

Abstract

The working part of Wiper Blades (WBs), made from PU material, are more vulnerable to contact-based solutions than other methods. In conventional approaches, sharp styluses employed as probes for tracking damaged edges are usually forced to wear out after a long time of the scanning process, thereby producing unreliable results. As a result, a machine vision-based system is proposed in this paper for WB damage inspection. Double threshold and morphological operations are used for defect verification. Defects are then derived using the background subtraction method before applying region-based algorithm for assessment. Results of experiments have demonstrated the reliability and flexibility of the new approach. Differences between the novel approach and the conventional method, which uses piezoelectric sensor, are also presented in this paper.

Introduction

In a ubiquitous society, there is an increasing demand for high quality printing, particularly the publication of newspapers, study materials, architecture and engineering drawings. Printer components such as the toner cartridge assembly may have a significant effect on the printing quality. Wiper Blades used in the manufacturing of toner cartridges have a strong influence on the resulting print quality of the toner cartridge. The quality of the WBs in turn is determined by the number of defects located on its edges. In addition, these defects are micro-dimension; therefore, they are too difficult to be recognized by the naked eyes. WBs, in toner cartridge remanufacturing processes, are also re-used up to 10 times for cost savings[1]. The average number of WBs necessary for daily re-production is approximately several thousand pieces, thus it is impossible to inspect them manually. Thus there is a demand for an automatic WB inspection system.

Andrij Harlan[1] invented a contact based WB inspection system and applied it in the re-manufacturing of monochromatic toner cartridge. The system includes three main functional assemblies: detector, transport system and assessment system. The detector, so-called stylus, slides on the edge of the WB edge with the transport system to detect damages along the edge. During the scanning process of the stylus, applied forces are generated between the stylus and the WB edge. These forces create equivalent voltage signals due to the physical characteristics of the piezoelectric film making up the stylus. These signals are then processed and evaluated by the assessment system which consists of a PC system and an amplifier. Places where defects appear, the signals are higher, thereby creating a rise in the -impulse. In the middle of the sliding process, generated signals are transferred to the amplifier, and processed signals are then sent to the CPU of the PC. When the scanning cycle ends, a relevant program, already installed in the PC, will show

the result and analysis of the WBs. Extremely high capacity is the prominent advantage of this method compared to other approaches. Additionally, micro-accuracy is also proposed as another advantage of this method. However, the method still has many drawbacks including fast worn-out stylus, false alarm and WB damage.

There are many papers written on noncontact-based method for defect inspection but none applied to WBs. Most of these papers are on inspection of fabric, textile, weld, etc[9]~[17]. In Gang Wang[9], used the subtraction background method for welding defect detection. The method; however, needs to construct an estimated background by an analytical software which increases the cost and complexity of the system. Besides, if noise reduction algorithms are not well-processed, there will have incorrect defects recognized as the correct ones. Ajay Kumar[10] proposed Linear Networks to detect fabric defects. The method needs a reference image, free of defects, to generate two 1-D projection signals which are used to calculate bias and weights of the network layer for deriving from estimated values. Defects are then collected from the deviation between the original signals (without-defect) and the estimated signals, current predicted values (with-defect). In spite of the low-cost system and the high-speed web inspection, the free-defect reference image is still required, the predicted signals are empirically identified, and the method fails to detect small objects which are micro-size. Similarly, G. M. Atiqur Rahaman and Md. Mobarak Hossain[16] employed some image processing techniques for detecting defects in ceramic tiles. The approach is quite simple and efficient; however, the requirement for reference image still remains. In comparison, Hongxia Liu et.al[17] used 2-D Wavelet Transform (2-D DWT) approach, in which template images are not necessary for defect detection of IC wafer. The method extracts the standard image, no defect, by applying 2-D DWT for three different IC images with the same layout. Defects are then found by making a comparison between each of defected IC image and the standard image. Despite the ability of application for two images in various lighting environment and especially robustness with that of condition, the method cannot be used for WBs.

Hence, we propose a new approach based on computer vision for WB inspection. The non-destructive method overcomes the drawbacks mentioned above for both the contact-based solution and the noncontact-based method. The application employs a VISIOMAR microscope-camera system, which composes of a MicrOkular sensor type (1/3"), electric LED lighting (5.5VDC, 200mA), USB interface for image acquisition, T400 Lenovo Laptop, Intel Core 2 duo, for programming and HP1320 WB for testing. Collected images are formatted as: color YUY2 TRUE COLOR, resolution 640x480, file type JPG. The camera saves a serial of image frames into a specific folder in the laptop hard disk; which are then accessed and evaluated by a Matlab-based program. Consequently, the program reads all the frames, converts them into gray scale, and thresholds these image frames before transferring the frames into binary images for further processing. Double threshold operation, background subtraction method, region-based algorithm and some other image processing techniques are used in the program to verify, detect and evaluate defects finally. This nondestructive inspection method avoids not only WB damage but also frequent calibration requirement. Additionally, it needs neither any extra software for background estimation nor template or reference image to implement the comparison with the original image. Alternately, the reference image is automatically generated by the program based on the background subtraction operation. Noises occurring after the binary images are created are completely removed by flood-fill operation and erasing algorithm for small regions. In addition, the method can not only detect defects of micrometer size but also quite convenient and reliable for WB inspection application. This approach is although dedicated to WB damage inspection, can also be applied to detect defect locations on straight edges of objects, particular in micro-size defects.

The experimental system model, detail principle explanation, experimental results and conclusions are presented in sections 2 to section 5 of this paper.

Experimental Inspection System

The experimental inspection system includes a camera system with a -software for data acquisition. The laptop is also equipped with a Matlab program for image processing technique applications and the carriage transmission for WB movement as shown in Figure 1.
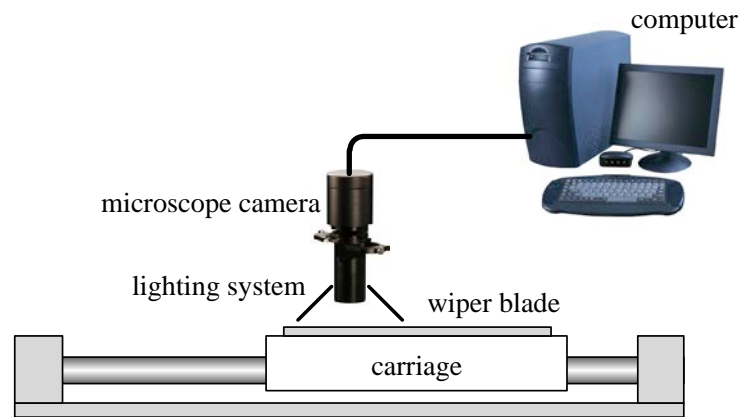

Figure 1. Experimental inspection system

The WBs must be cleaned and left in a pure atmosphere for drying before being scanned under the camera lens. The carriage is manually moved step by step so that the camera can take each frame of image sequentially. The overall system magnification is approximately 1200x, and calculated pixel size is 0.2μm. The value of each moving step is 0.128mm equivalent to the width of each image frame. In the experiment, we just consider HP1320-WB whose working edge is 210mm length. The total number of taken frames is therefore 1641. All image frames are saved in a specific location in the laptop for further process. Subsequently, the Matlab program reads the frames automatically to perform the assessment of the WB. In the next section, algorithms used in the program for image processing are explained in detail.

Principle of Automatic Detection

The section is respectively divided into three subheadings, defect specification, image threshold and image processing. The detailed explanations of each part are presented as follows.

- Camera sensor format: 1/3"
- Camera pixel size: 0.2μm
- Electric LED lighting: 5.5VDC, 200mA
- Camera interface: USB

Defect Specification

Based on an empirical study, the specifications of the HP1320-WB are established as below.

- Smallest defect will be counted if its size is more than or equal 7 pixels in height and width for each dimension.

- Yellow threshold is lower limit which allows up to 700 pixels of defects overall reaching for each WB. If the total defected pixels exceed this number, the WB will be rejected.
- Red threshold is upper limit which allows no defect reaching. The width for this type of defects is at least 50 pixels for every significant damage.
- Working edge of the WB is 210mm length in the middle alignment. Any part of the WB outside this range is neglected because of the effect on of the print.

Image Threshold

Firstly, the acquired images are converted into gray-scale type. They are then segmented by the Otsu threshold method available in the Matlab Image Processing Toolbox. Figure 2 shows the Otsu algorithm.
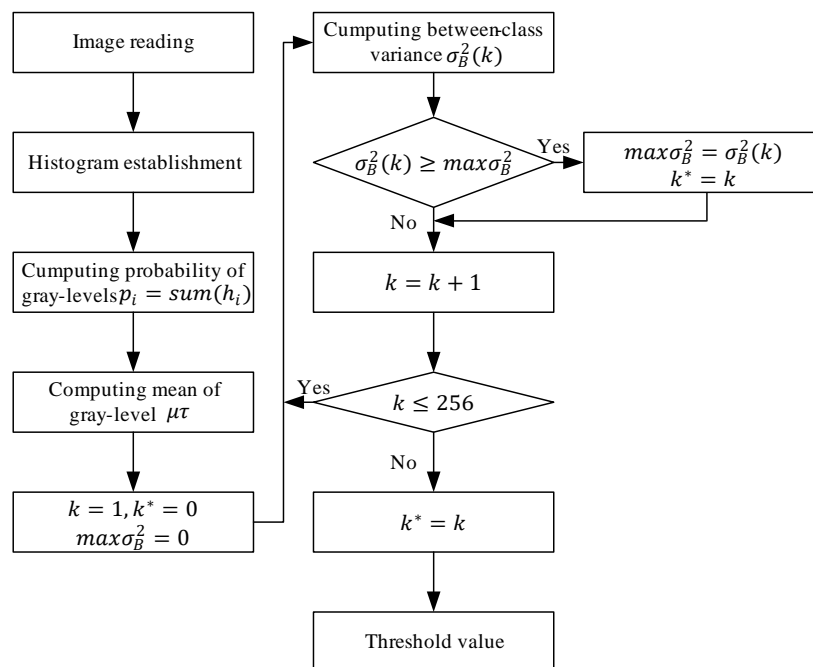

Figure 2. Otsu threshold flow chart[18]

Image Processing

After getting the binary images in the previous step, we start processing them by the following procedures.

Remove False Regions

Some false regions still remain due to the lighting problem at the defect positions so it must be removed for further process. Figure 3 and Figure 4(b) represent the block diagram of the operation and the output image after removal respectively.
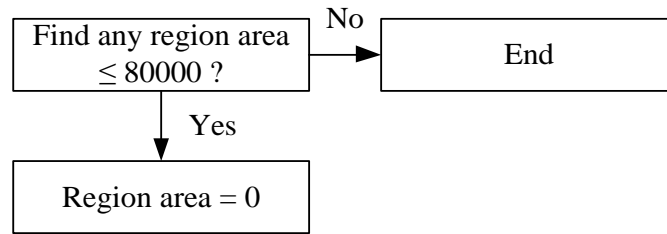
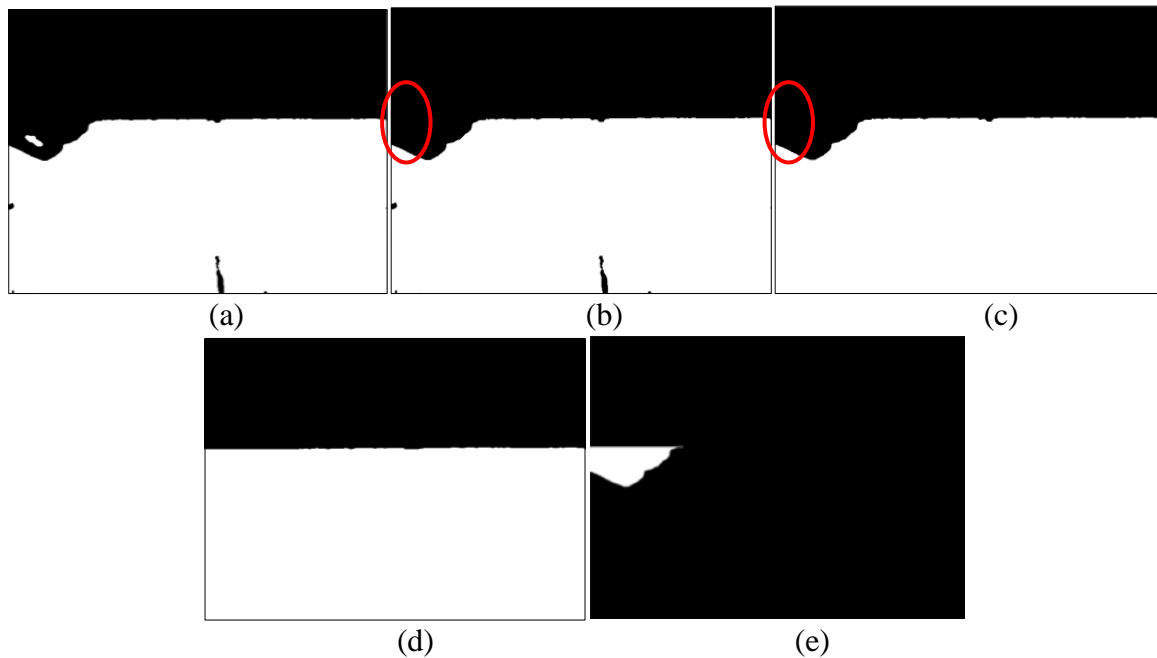Figure 3. Removed False Regions – Block Diagram

Figure 4. (a) Binary threshold image (b) false regions removed (c) last column treatment
(d) binary mask image and (e) defected region found (Scale: 351x)

Treat First and Last Column of Image Frame

The first and last column of the image frames occasionally have noises therefore they need to be treated. Define:

r_1, r_2: the row of first located pixel in first and second column respectively.

f (i, j): the pixel value at coordinate x = i and y = j
Then: $\forall\ i \in [r_1, r_2]$,

$$f(i, 1) = \begin{cases} f(i,1), & f(i,1) = f(i,2) \\ f(i,2), & f(i,1) \neq f(i,2) \end{cases} \tag{1}$$

Figure 4(b) presents an example of the last column problem, and Figure 4(c) shows how the problem is treated by (1).

Remove Impurities

It is rather difficult to get rid of contaminations by preprocessing the WB before making the experiment. Stains are left on the WB surface after cleaning; therefore, it is necessary to remove them. This can be done by using the flood-fill operation[2].

Let *f(x,y)* describe binary image and suppose that we choose marker image, *fm(x,y)*, to

be 0 everywhere except for the places on the image border, where it is set to 1- f:

$$f_m(x,y) = \begin{cases} 1 - f(x,y), \ if \ is \ on \ the \ border \ of \ f \\ 0, \ otherwise \end{cases} \qquad (2)$$

Then,

$g = [R_f c(f_m)]^c$ has the defect of filling the holes in f.

Figure 4(c) denotes impurities removed after applying (2).

Defect Verification

The double threshold method is used for segmenting the reflected light at the damaged positions on the WB edge. If the gray-level values of the defect zones are in range of the threshold, the damaged areas will be represented by white pixels until the edge. This edge will be described as an incline line if its thickness found by the method is no more than 5 pixels. Pseudo-defects are neglected for other cases.

$$g(x,y) = \begin{cases} 1, \ if \ T_1 \leq f(x,y) \leq T_2 \\ 0, \ otherwise \end{cases} \qquad (3)$$

where,

$g(x,y)$: output image

$f(x,y):$ gray-scale image

T_1, T_2 : lower and upper threshold values

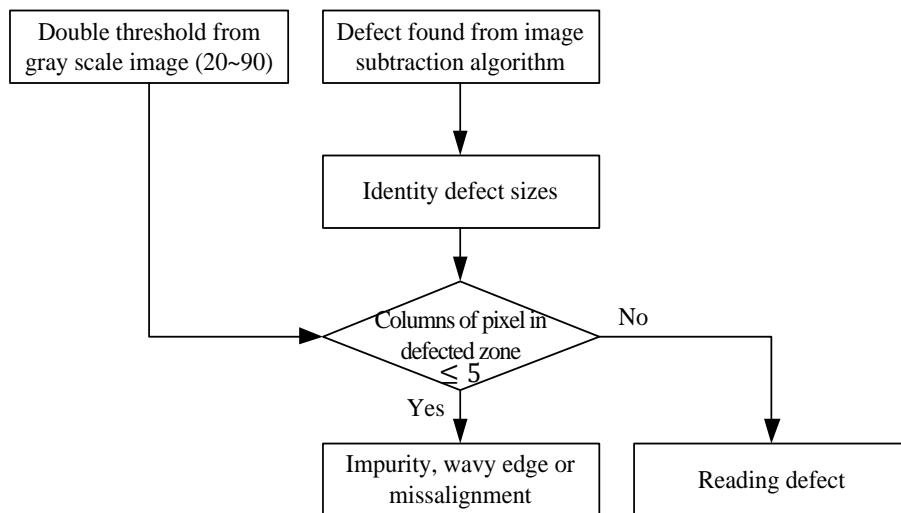The algorithm diagram of defect verification process is shown as Figure5.

Figure 5. Defect verification algorithm

The problem of misalignment and real defect detection are presented in Figure 6 and Figure 7 respectively.

Misalignment problem is treated by neglecting found regions whose height is no more than five pixels as shown in Figure 6.

Defect regions after detected are recorded with dimensions and locations. At considerable damaged zones, defects are brighter due to diverged lighting phenomenon. However, these bright areas are quite discrete, Figure 7(c). Therefore, morphological

operation is used for gathering these areas in accordance with the boundary of the WB edge, Figure 7(d). Eventually, white pixels representing damaged regions are displayed in the form of columns, and real defects are identified as shown in Figure 8.
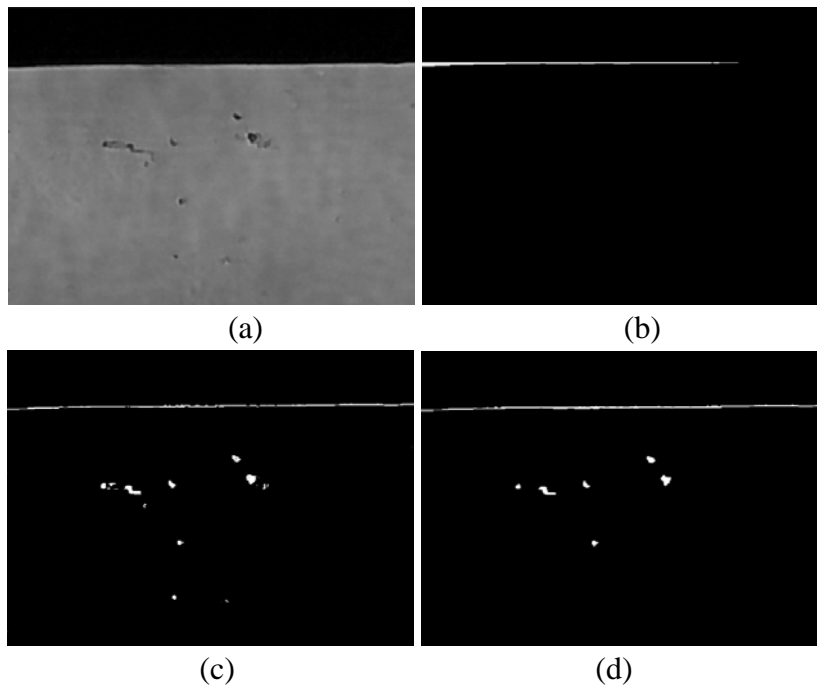

(a)

(b)

(c)

(d)

Figure 6. Mistaken defect detection due to misalignment (a) gray-scale image,
(b) misaligned region, (c) double threshold, (d) morphological application (scale: 367x)
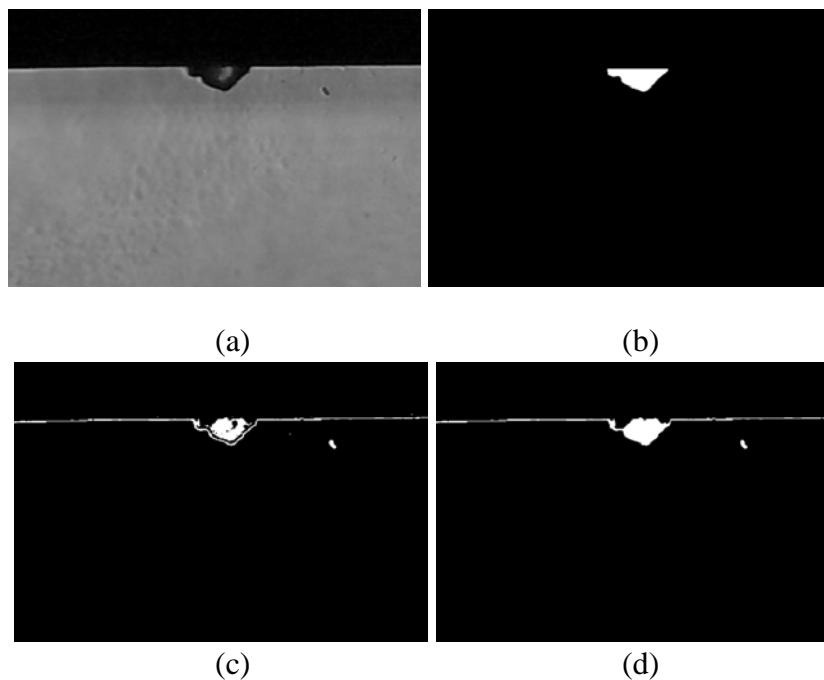

(a)

(b)

(c)

(d)

Figure 7. Real defect detection (a) gray-scale image, (b) defect zone, (c) double
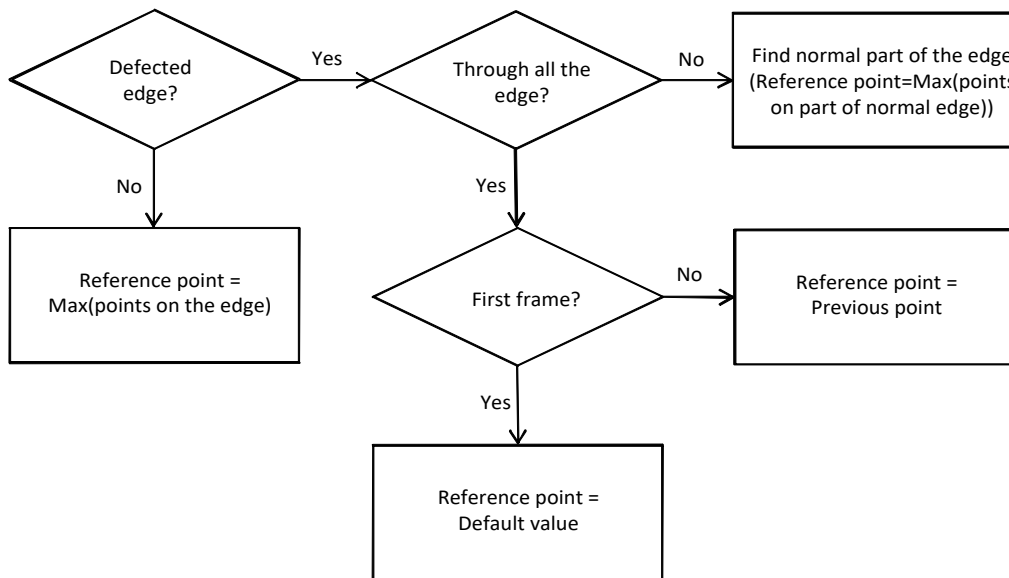threshold, (d) morphological application (scale: 367x)

Figure 8. Algorithm diagram for deriving reference line

Defect Detection

After the defects are verified, the reference points of the image frames are searched for the reference line. Image subtraction technique is then applied for defect detection. It would be simple if defects are located in the middle of the WB edge or appears within one image frame. In fact, there are totally 1641 image frames, additionally, defects may occur at any frame located at any place of the WB edge. It might be even through all the length of the frames. Hence, an algorithm is proposed as shown in Figure 8 to solve this problem.

After getting these reference points, we can identify the reference lines easily by drawing horizontal lines of pixels 1 (from left-most to right-most of the image frames). These lines also called virtual working edges are used to produce mask images later.

Defects are found as presented in Figure 4(e) by subtracting the processed image frame from the mask image. The generation of the mask image, Figure 4(d), is implemented in the same way as the impurities removal in the previous step.

Defect Location and Final Assessment

Region-based algorithm is used for this process. Firstly, all defects in the image frames are labeled in top-down and left-right order of priority. Then, each label is identified and contains the important information such as location, width and height for evaluation.

In the algorithm, defects are described by columns of pixel 1 next to each other. Figure 9 illustrates how the algorithm locates and measures defected regions.
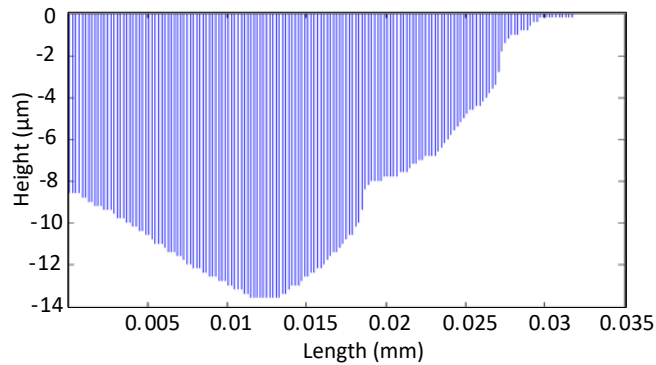
Figure 9. Defect region illustrated by bolumns of pixel (scale: 1900x)

The WB is automatically judged pass or fail depending on whether or not the tested WBs meet the conditions as mentioned in part A of section III.

Experimental Results

Defect detection and final assessment are two crucial factors needed to be investigated. Therefore, we consider them as the main parts of the inspection results. Labeling 3 pieces of the WB from 1 to 3, our target is to use the novel algorithm for automatically evaluating how many defected image frames have taken place, how significant the defects affect the quality of print page, and the reliability of the algorithms when compared to the conventional method.

For calculating the total number of defect frames, we manually checked one by one the acquired image frames and classify real defects according to predetermined specifications. The frames compared with the automatically detected defects. As a result, we obtain true and false detection rate as Table 1.

Table 1. Detection Performance

Sample No	Image Frame				
	Total Defects	Total Detected Defects	Total Correct Detected Defects	Detection Ratio (%)	Mistaken Detection Ratio (%)
1	147	140	136	92.5	2.7
2	190	190	185	97.4	2.6
3	585	584	568	97.1	2.7

For judging the influence of damages on the WB edge and the reliability of the proposed algorithms, a comparison between our method and piezoelectric solution is implemented. We tested the same pieces of the WB for both our approach and the piezoelectric method, and the results are compared is shown as Table 2.

These WBs are tested on the same toner cartridge and printer for checking the quality of print page. Figure 10, 11 and 12, 13 represent the WB edge analysis diagrams and the effect of damages on print-page quality for Sample 1 and Sample 2 respectively. The edge processing map of Sample 3 is also displayed in Figure 14.

Table 2. Inspection Performance In Comparison

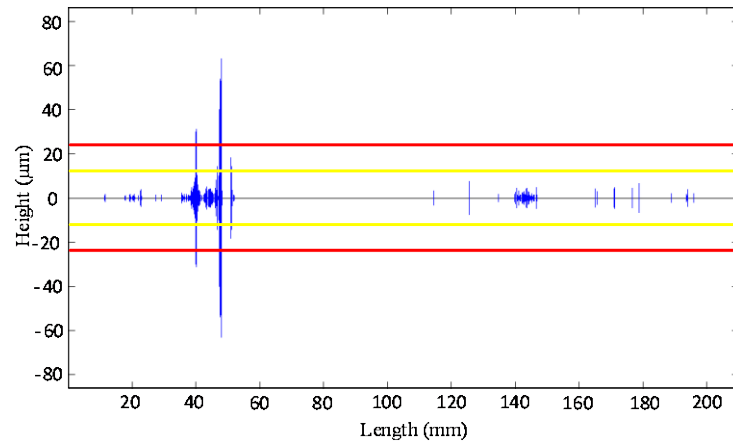| Sample No	Damage Inspection				
	Yellow Limit Exceeded	Red Limit Exceeded	Print Page Result	New Method Assessment	Piezoelectric-based Method Assessment
1	Yes	Yes	Fail	Fail	Fail
2	Yes	Yes	Fail	Fail	Pass
3	Yes	No	Pass	Fail	Pass

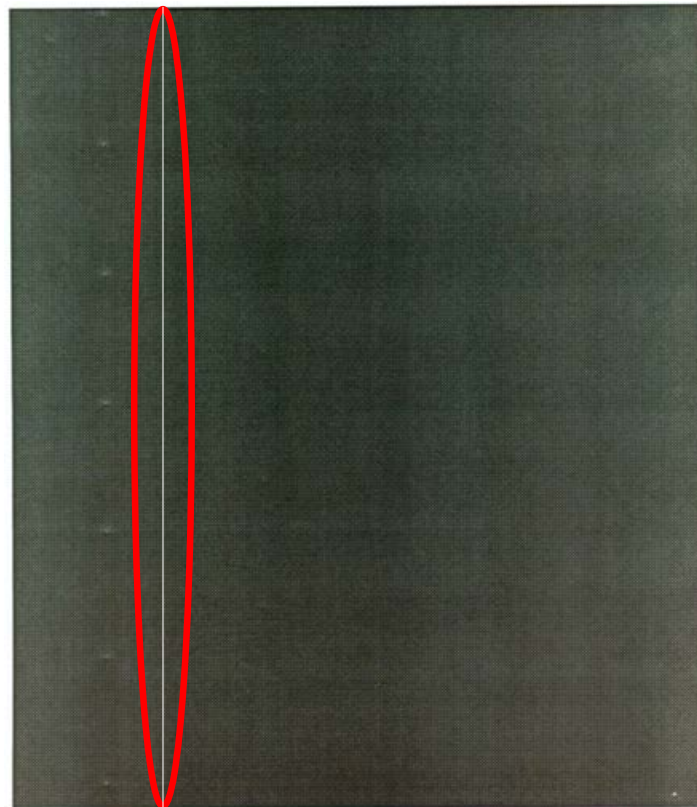Figure 10. WB edge analysis diagram – sample 1 (scale: 0.41x)

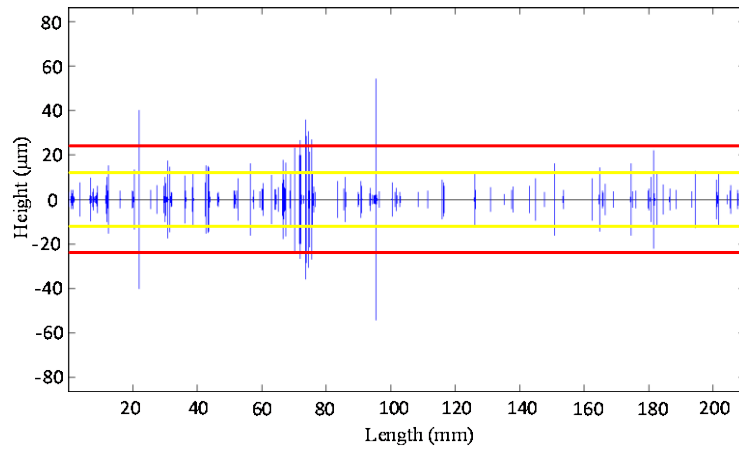Figure 11. Print page result – sample 1 (scale: 0.41x)

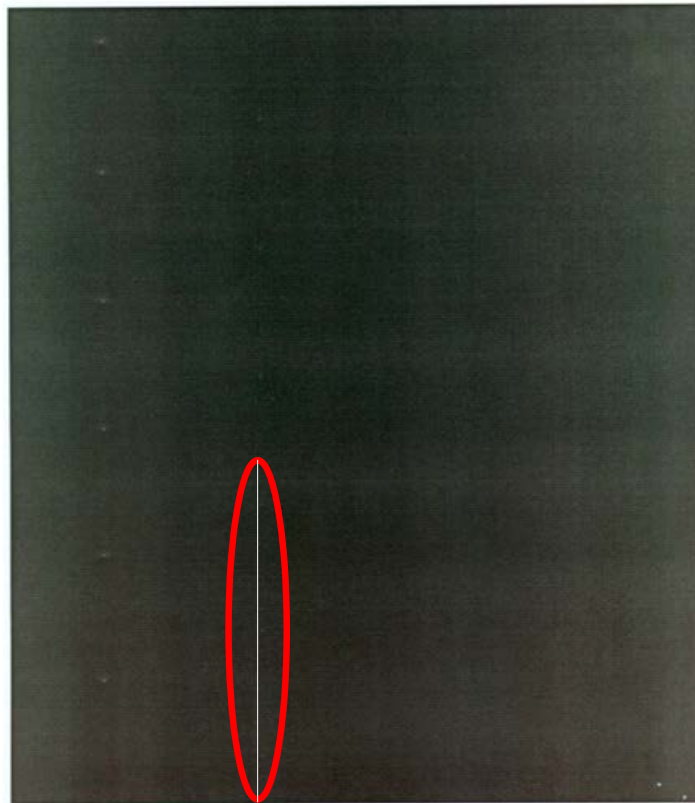Figure 12. WB edge analysis diagram – sample 2 (scale: 0.41x)

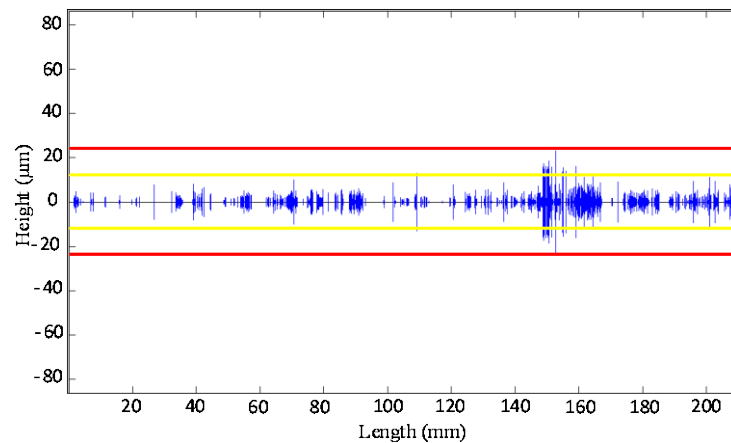Figure 13. Print page result – sample 2 (scale: 0.41x)

Figure 14. WB edge analysis – sample 3 (scale: 0.41x)

The defect recognition ratio, over 92%, demonstrated the efficiency and reliability of the new method. The error detection ratio of 2.7% for the highest, means that misalignment, wavy edge and impurity problems have been successfully solved by applying the double threshold algorithm. Nevertheless, there still remain recognition errors mainly due to noise sources from the other side of the tested edges. Besides, detection errors are also added by the algorithm, specifically in this case, it is 7 pixels (0.2μm/pixel). While the recognition error can be removed by enhancing the lighting intensity and carefully clean the WB edge, the algorithm error can be minimized by decreasing the number of pixel of sensitivity adjustment. The more sensitive the algorithm (the lower number of pixel), the smaller detectable size of defects, but the longer time for processing is required. However, it is experimentally proven that if damage width or depth is no more than 7 pixels, the damage is very slight and can be neglected.

Conclusions

Defect detection rate is high enough for demonstrating the reliability of the new approach. Noncontact-based method is much safer for WB testing and less time required for calibration. The algorithm is flexible since we can adjust the sensitivity of the defect detection probability. The method does not demand for either template or reference images, the reference line formation is reliably built in the algorithms instead. In addition, detectable size of defects in the method is 1.4μm, which is suitable for micro-size damage evaluation. The method is dedicated for WB damage inspection applications. For different kinds of WB, it is necessary to adjust some parameters in the algorithms corresponding with various required specifications. Besides, the method is applicable for examining micro-defects locating on straight edge of one object along its length.

One of the significant factors, capacity, which makes the new method applicable to toner cartridge re-manufacturing industries, has not been satisfied yet. Average time needed for each test is from several decades of second to over two minutes. It is, therefore, essential to develop the program from Matlab environment into C platform and set up mechanical modification properly for obtaining real-time processing.

Reference

[1] A. Harlan, *Wiper Blade Assessment System and a Method Thereof.* United States patent 6792387 B2. 2004-9-14, 2004.

[2] R.C. Gonzalez, R.E. Woods, and S.L. Eddins, *Digital Image Processing Using Matlab*, Gatesmark Publishing, Knoxville, TN, United States 2003.

[3] R.C. Gonzalez, and R.E. Woods, *Digital Image Processing*, Prentice Hall, Upper Saddle River, NJ, United States 2002.

[4] A. McAndrew, *An Introduction to Digital Image Processing with Matlab*, Victoria University of Technology, Melbourne, Australia, 2004.

[5] N. Otsu, "A threshold selection method from gray-level histograms," *IEEE Transaction on Systems, Man and Cybernetics*, Vol. 9, No. 1, pp. 62-66, 1979.

[6] N. Papamarkos, and B.Gatos, "A new approach of multilevel threshold selection," *Graphical Models and Image Processing*, Vol. 56, No. 5, pp. 357-370, 1994.

[7] L. Song, X. Qu, K. Xu and L. Lv, "Three dimensional measurement and defect detection based on single image," *Journal of Optoelectronics and Advanced Materials*, Vol. 7, No. 2, pp.1029-1038, 2005.

[8] J.S. Song, K. Maghsoudi, W. Li, E. Fox, J. Quackenbush, and X.S. Liu, "Microarray blob-defect removal improves array analysis," *Bioinformatics*, Vol. 23, No. 8, pp. 966-971, 2007.

[9] G. Wang, and T.W. Liao, "Automatic identification types of welding defects in radiographic images," *NDT&E International*, Vol. 35, No. 8, pp. 519-528, 2002.

[10] A. Kumar, "Neural network based detection of local Textile defects," *Pattern Recognition*, Vol. 36, pp. 1645-1659, 2003.

[11] Y. Sun, P. Bai, H.-Y Sun, and P. Zhou, "Real-time automatic detection of weld defects in steel pipe," *NDT&E International*, Vol. 38, No. 7, pp. 522-528, 2005.

[12] S.H. Choi, J.P. Yun, B. Seo, Y.S. Park, and S.W. Kim, "Real-time defects detection algorithm for high-speed steel bar in coil," *World Academy of Science, Engineering and Technology*, Vol. 25, pp. 66-70, 2007.

[13] N.K.A. Khalid, Z. Ibrahim, and M.S.Z. Abidin, "An algorithm to group defects on printed circuit board for automated visual inspection," *IJSSST*, Vol. 9, No. 2, pp. 1-10, 2008.

[14] K.L. Mak, P. Peng, and K.F.C. Yiu, "Fabric defect detection using morphological filters," *Image and Vision Computing*, Vol. 27, pp. 1585-1592, 2009.

[15] S. Kabir, P. Rivard, D.-C. He, and P. Thivierge, "Damage assessment for concrete structure using image processing techniques on acoustic borehole imagery," *Construction and Building Materials*, Vol. 23, pp. 3166-3174, 2009.

[16] G.M.A. Rahaman, and Md.M. Hossain, "Automatic defect detection and classification technique from image: A special case using ceramic tiles," *International Journal of Computer Science and Information Security*, Vol. 1, No. 1, pp. 22-30, 2009.

[17] H. Liu, W. Zhou, Q. Kuang, L. Cao, and B. Gao, "Defect detection of IC wafer based on two-dimension wavelet transform," *Microelectronics Journal*, Vol. 41, pp. 171-177, 2010.

[18] T.D. Tran and T.H. Bui. *Nghien Cuu Phuong Phap Xu Ly Anh Ung Dung Trong Dieu Khien Chinh Xac Vi Tri Board Mach Dien Tu.* Thesis (B.S), Ho Chi Minh City University of Technology, Ho Chi Minh City, Vietnam, 2008.